ELSEVIER

Physica D 100 (1997) 311–329

PHYSICA D

Renormalization and transition to chaos in area preserving nontwist maps

D. del-Castillo-Negrete *, J.M. Greene [1], P.J. Morrison

Department of Physics and Institute for Fusion Studies, The University of Texas at Austin, Austin, TX 78712, USA

Received 29 Febuary 1996; revised 13 August 1996; accepted 13 August 1996
Communicated by J.D. Meiss

Abstract

The problem of transition to chaos, i.e. the destruction of invariant circles or KAM (Kolmogorov–Arnold–Moser) curves, in area preserving *nontwist* maps is studied within the renormalization group framework. Nontwist maps are maps for which the twist condition is violated along a curve known as the shearless curve. In renormalization language this problem is that of finding and studying the fixed points of the renormalization group operator $\mathcal{R}$ that acts on the space of maps. A simple period-two fixed point of $\mathcal{R}$, whose basin of attraction contains the nontwist maps for which the shearless curve exists, is found. Also, a critical period-12 fixed point of $\mathcal{R}$, with two unstable eigenvalues, is found. The basin of attraction of this critical fixed point contains the nontwist maps for which the shearless curve is at the threshold of destruction. This basin defines a new universality class for the transition to chaos in area preserving maps.

1. Introduction

A fundamental problem of Hamiltonian dynamics is to understand the behavior of an integrable Hamiltonian system when subject to perturbation. In terms of the action–angle variables (J, θ) of the integrable system, the Hamiltonian for the perturbed system in the case of one degree-of-freedom can be written as

$$H = H_0(J) + H_1(J, \theta, t), \tag{1}$$

where H_0 is the Hamiltonian of the integrable system and the perturbation is represented by H_1. Since the pioneering work of Poincaré, it has been known that the dynamics for Hamiltonians of this form is far from trivial. Typically, the phase space consists of a complicated mixture of integrable (confined to invariant tori) and nonintegrable (chaotic) trajectories. Thus, the problem of the transition to chaos is to determine which trajectories of H_0 remain integrable and which become chaotic under the effect of H_1.

* Corresponding author. Present address: Scripps Institution of Oceanography 0230, University of California at San Diego, La Jolla, CA 92093-0230, USA. E-mail: diego@fawlty.ucsd.edu.

[1] Present address: General Atomics Inc., San Diego, CA 92186–9784, USA.

PII S0167-2789(96)00200-X

When the perturbation is periodic in time, i.e. $H(J, \theta, t+T) = H(J, \theta, t)$, the essential aspects of the dynamics are captured by the so-called Poincaré map, which is obtained by plotting the phase space coordinates of the trajectories at times $t = T, 2T, 3T, \ldots, nT, \ldots$ Since, in general, Hamilton's equations preserve the volume of phase space, the Poincaré map is an area preserving map. Accordingly, the behavior of Hamiltonian systems can be understood by studying area preserving maps, which are relatively simpler mathematical objects than differential equations (see for example [1–3] and references therein). In particular, the transition to chaos for Hamiltonians of the form of Eq. (1) can be studied with area preserving maps of the form

$$x_{i+1} = x_i + \Omega(y_{i+1}) + f(x_i, y_{i+1}), \qquad y_{i+1} = y_i + g(x_i, y_{i+1}), \tag{2}$$

where the area preservation condition requires $\partial f/\partial x_i + \partial g/\partial y_{i+1} = 0$. The map variables (x, y) correspond to the action–angle coordinates (J, θ), the function Ω corresponds to the unperturbed frequency $\partial H_0/\partial J$, and the functions f and g correspond to the perturbation H_1.

When f and g are zero the map is integrable: successive iterations of initial conditions lie on straight horizontal lines that wrap around the periodic x-domain. The *rotation number* of an orbit is defined, when it exists, by $\omega := \lim_{i\to\infty} x_i/i$, where in this definition the x-coordinate is lifted to the real line (i.e. x is not taken to be periodic). Orbits with irrational rotation numbers fill one-dimensional dense sets called invariant tori (circles) or KAM (Kolmogorov–Arnold–Moser) curves. On the other hand, periodic orbits have rational rotation numbers. Under the effect of the perturbation some KAM curves are broken whereas others are merely deformed – they remain topologically equivalent to straight lines. The problem of the transition to chaos in area preserving maps is to determine which KAM curves persist and which are destroyed by a nonintegrable perturbation of the map.

In the present paper we study the transition to chaos in the following area preserving map:

$$x_{i+1} = x_i + a(1 - y_{i+1}^2) \tag{3}$$

$$y_{i+1} = y_i - b \sin(2\pi x_i), \tag{4}$$

where a and b are real numbers, and the domain of interest is $D := \{(x, y) \mid y \in (-\infty, \infty) \text{ and } x \in (-\frac{1}{2}, \frac{1}{2}) \bmod 1\}$. Following the terminology of [4], we call this map the *standard nontwist map* because it violates the *twist condition*,

$$\frac{\partial x_{i+1}}{\partial y_i} \neq 0, \tag{5}$$

which is the map analog of the *nondegeneracy condition* for Hamiltonian systems,

$$\frac{\partial^2 H_0}{\partial J^2} \neq 0. \tag{6}$$

The point where the twist condition fails can be an extremum (if $\partial x_{i+1}/\partial y_i$ changes sign), as in the case of the standard nontwist map, or an inflection point (if $\partial x_{i+1}/\partial y_i$ does not change sign). The most interesting and challenging case, the one addressed here, is that of an extremum.

The study of the transition to chaos in area preserving nontwist maps, and equivalently in degenerate Hamiltonian systems, is a problem of both theoretical and practical relevance. Mathematically the problem is of interest because many results in the theory of area preserving maps, including the KAM theorem [5], depend upon the twist condition. Recently there have been attempts to extend KAM theory to nontwist maps [6]. From a physics perspective, degenerate Hamiltonian systems and nontwist maps are important because such systems naturally occur in a variety of problems of fluid dynamics, plasma physics, celestial mechanics, accelerator physics, condensed matter physics, and ray optics in wave guides, among others. (For a discussion of some of these applications see [7,8].)

For $b = 0$ the standard nontwist map is integrable. In this case, the twist condition is violated along the line $y = 0$, which we call the *shearless curve* because along it the shear, $\partial x_{i+1}/\partial y_i$, vanishes. A precise and general (for a and b nonzero) definition of the shearless curve is given in Section 2. As a and b deviate from zero, the shearless curve bends and eventually breaks. The problem of transition to chaos in nontwist maps is to understand when and how this shearless curve breaks. Here we study this problem, restricting attention to the case in which the rotation number of the shearless curve is equal to the inverse golden-mean, $1/\gamma := \frac{1}{2}(\sqrt{5} - 1)$.

The transition to chaos in area preserving maps exhibits *critical scaling* behavior [9,10]. This means that at the threshold of its destruction (i.e. at criticality), a KAM curve possesses nontrivial scaling properties. In particular, critical KAM curves are fractals, well-known geometrical objects that remain invariant under appropriate successive spatial rescalings. These scaling properties are believed to be universal in the sense that they depend only on very general features of the map. In a way akin to what is done in the theory of phase transitions, one can introduce *universality classes* for classifying the fundamentally different ways in which the transition to chaos can take place. These universality classes group together all the maps that share the same scaling properties at criticality, even though the maps might "look" different. Thus, a fundamental problem is to determine the possible universality classes of the transition to chaos in area preserving maps. In [11–13] it was shown that this problem can be studied using renormalization group techniques.

The goal of renormalization in area preserving maps is to provide a framework for the study of a KAM curve with a given rotation number. It is important to note that while KAM theory deals with the persistence of dense sets of invariant curves, the renormalization approach deals only with individual KAM curves of prescribed rotation numbers. This loss of generality is compensated for by a gain in precision: renormalization group estimates for the persistence of a KAM curve are considerably better than estimates provided by KAM theory, which are generally too conservative.

The basic idea of renormalization is embodied in the *renormalization group operator* $\mathcal{R}$, which maps the function space of area preserving maps into itself. Iteration of this operator, which takes an area preserving map into another such map, enables one to study a KAM curve on successively smaller spatial scales and successively longer time scales. From this "space–time zooming" the fate of the KAM curve can be determined. More formally, the destruction or persistence of the KAM curve of a map M is determined by the asymptotic behavior of $\mathcal{R}$ acting repeatedly on M. As will be explained in Section 3, the asymptotic behavior of the operator $\mathcal{R}$ is largely determined by its fixed points, which are maps invariant under renormalization. Thus, in renormalization language, the problem of transition to chaos corresponds to the problem of finding and studying critical fixed points of $\mathcal{R}$. Since the discovery of the critical period-one fixed point for twist maps [11,12], other fixed points have been found in standard *twist* maps [14–19]. In the present paper, we demonstrate the existence of a new, higher order, critical fixed point of the renormalization operator: the one associated with the transition to chaos of the $1/\gamma$ KAM shearless curve that occurs in nontwist maps. This fixed point has two unstable eigenvalues. We also show that the simple fixed point for nontwist maps is a period-two fixed point of $\mathcal{R}$.

In Section 2, we review previous results on the transition to chaos in the standard nontwist map [7,8] and study the spatial scaling properties of the shearless curve at criticality. In Section 3, after reviewing the renormalization group formalism, we discuss the simple and critical fixed points corresponding to nontwist maps, and compute the two unstable eigenvalues of the critical fixed point. Section 4, contains the conclusions. The present work is based in part on [7].

2. Transition to chaos

In this section we consider the destruction of the shearless curve. Section 2.1, contains the summary of previous results, while Section 2.2, contains the discussion of the spatial scaling properties of the shearless curve at criticality.

2.1. Summary of previous results

The analysis of the transition to chaos requires the use of periodic orbits. Therefore, we review here our previous results on periodic orbits in the standard nontwist map [7,8].

A point $\boldsymbol{x} := (x, y)$ generates a *periodic orbit* of *order n* if after n iterations it returns to itself; i.e. $M^n\boldsymbol{x} = \boldsymbol{x}$. The rotation number associated with a periodic orbit is the rational number m/n, where n is the order of the periodic orbit and m is the integer number of times the orbit cycles through the x-domain before returning to its initial position. The standard nontwist map is reversible and accordingly can be decomposed into a product of involutions: $M = I_1 I_0$, where $I_0\boldsymbol{x} := (-x, y - b\sin(2\pi x))$ and $I_1\boldsymbol{x} := \big(-x + a(1 - y^2), y\big)$. The invariant sets of the involution maps, $\mathcal{I}_{0,1} := \{\boldsymbol{x} | I_{0,1}\boldsymbol{x} = \boldsymbol{x}\}$, form the *symmetry lines* of the map. For the standard nontwist map, $\mathcal{I}_0$ is the union of the following symmetry lines:

$$s_1 = \{(x, y) \mid x = 0\}, \qquad s_2 = \{(x, y) \mid x = \tfrac{1}{2}\}, \tag{7}$$

while the invariant set $\mathcal{I}_1$ is the union of

$$s_3 = \{(x, y) \mid x = \tfrac{1}{2}a(1 - y^2)\}, \quad s_4 = \{(x, y) \mid x = \tfrac{1}{2}a(1 - y^2) + \tfrac{1}{2}\}. \tag{8}$$

Symmetry lines reduce the search for periodic orbits to a one-dimensional root finding problem, which is described further in [7,8].

Because of the violation of the twist condition, periodic orbits in the standard nontwist map come in pairs; that is, contrary to what happens typically in twist maps, there are *two* periodic orbits with the *same* rotation number on each symmetry line. This is evident when $b = 0$, in which case periodic orbits with rotation number m/n on s_1, for example, are located at $(0, \pm\sqrt{1 - (m/n)/a})$. We call the periodic orbit with the larger y-coordinate the *up* orbit and that with the smaller y-coordinate the *down* orbit. As the map parameters are varied the up and down periodic orbits on a symmetry line can collide giving rise to a rich variety of bifurcations including separatrix reconnection, a global bifurcation that changes the phase space topology in the vicinity of the shearless curve. At the collision point, the residue (cf. [20]) and the Poincaré index of the up and down periodic orbits vanish.

Given a rational number r/s, the r/s *bifurcation curve*, $b := \boldsymbol{\Phi}_{r/s}(a)$, is defined as the locus of points (a, b) for which the r/s periodic orbits are at the point of collision. Given an irrational number σ, and a sequence of rational numbers $\{r_i/s_i\}$ such that $\lim_{i\to\infty} r_i/s_i = \sigma$, the σ *bifurcation curve* is defined by $b = \boldsymbol{\Phi}_\sigma(a) := \lim_{i\to\infty} \boldsymbol{\Phi}_{r_i/s_i}(a)$. By construction, for (a, b) values below $\boldsymbol{\Phi}_\sigma$ all the periodic orbits with rotation numbers $r/s < \sigma$ are below their collision point and thus exist and can be found by using the symmetry line formalism.

Given two integer numbers r and s, an r/s *nontwist map* is defined as a map satisfying the following two conditions: (i) The map has either no periodic orbits with rotation number greater than r/s, or it has no periodic orbits with rotation number less than r/s. (ii) The map does have periodic orbits with rotation number equal to r/s, and these orbits have zero residue and zero Poincaré index. The condition on the Poincaré index is imposed to ensure that the zero residue periodic orbits are at the bifurcation point where the up and down periodic orbits have collided. Bifurcation curves can be used to construct σ nontwist maps, where σ is either a rational or an irrational number. In particular, the standard nontwist map with (a, b) values restricted to the σ bifurcation curve is a one-parameter σ nontwist map.

For a σ nontwist map, a *shearless curve* is defined as a curve with rotation number equal to σ. Throughout this (and the previous [8]) paper we concentrate on the study of the $1/\gamma$ shearless curve. This curve, when it exists, can be found approximately as follows: First, construct an approximation to the $\boldsymbol{\Phi}_{1/\gamma}$ bifurcation curve; this was done by computing $\boldsymbol{\Phi}_{F_i/F_{i+1}}$ for Fibonacci ratios F_i/F_{i+1} up to $75,025/121,393$, and by using the scaling relation of Eq. (41). Using this, the $1/\gamma$ shearless curve can be approximated for an (a, b) value on $\boldsymbol{\Phi}_{1/\gamma}$ by the

set of up and down periodic orbits with rotation numbers $\{F_{2i-1}/F_{2i}\}$; we considered rational approximants up to 46, 368/75, 025.

To compute the critical (a, b) values for the destruction of the shearless curve we used the residue criterion [20], according to which a KAM curve exists (does not exist) if the residues of the periodic orbits approximating it converge to zero (infinity). The parameter value(s) at which the residues exhibit a nontrivial convergence (i.e. $\neq 0, \infty$) defines the critical point. Employing the residue criterion, we found in [7,8] that the critical point for the destruction of the $1/\gamma$ shearless curve in the standard nontwist map is:

$$(a_c, b_c) = (0.686049,\ 0.742493131039). \tag{9}$$

At this critical value, the residues of the down periodic orbits on s_1 and s_4, as well as the residues of the up periodic orbits on s_2 and s_3 converge to the *six-cycle* $\{H_1, H_2, H_3, H_4, H_5, H_6\}$ where:

$$H_1 = 2.325 \pm 0.002, \qquad H_2 = 2.575 \pm 0.020, \tag{10}$$

$$H_3 = -0.599 \pm 0.010, \qquad H_4 = -1.283 \pm 0.001, \tag{11}$$

$$H_5 = 2.575 \pm 0.020, \qquad H_6 = 1.548 \pm 0.037. \tag{12}$$

On the other hand, the residues of the up periodic orbits on s_1 and s_4, as well as the residues of the down periodic orbits on s_2 and s_3 converge to the six-cycle $\{H_1, -H_2, H_6, H_4, -H_5, H_3\}$.

2.2. Spatial scaling at criticality

Now consider the spatial scaling of the shearless curve at criticality. To this end it is convenient to introduce *symmetry line coordinates*,

$$\hat{x} := x - \tfrac{1}{2}a(1 - y^2), \qquad \hat{y} := y - y_s, \tag{13}$$

where y_s is the y-coordinate of the point where the shearless curve intersects the s_3 symmetry line. In these coordinates, the s_3 symmetry line becomes a straight line that intersects the shearless curve at the origin.

Fig. 1(a) shows, in symmetry line coordinates, a portion of the $1/\gamma$ shearless curve at criticality. Fig. 1(b) shows a magnification, centered at the origin, of Fig. 1(a); the x-coordinate is scaled by a factor of 321.92 and the y-coordinate is scaled by a factor of 463.82. The spatial self-similar (fractal) structure of the $1/\gamma$ shearless curve at criticality is displayed by the remarkable similarity between Figs. 1(a) and (b). To understand the origin of this self-similarity, up periodic orbits with rotation numbers 55/89 and 17 711/28 657 are shown in Fig. 2(a), again using symmetry line coordinates. (Equivalent results are obtained for down periodic orbits.) In this figure, the circles denote the coordinates of the 55/89 up periodic orbit, while the crosses denote the coordinates of the 17 711/28 657 up periodic orbit after the spatial rescaling $(\hat{x}, \hat{y}) \to (321.92\,\hat{x},\ 463.82\,\hat{y})$. A similar plot is presented in Fig. 2(b), where the 144/233 up periodic orbit (circles) is plotted along with the spatially rescaled 46 368/75 025 up periodic orbit (crosses). From Fig. 2(a) ((Fig. 2(b)) it is seen that if the spatial coordinates are rescaled then, close to $(\hat{x}, \hat{y}) = (0, 0)$, a periodic orbit with rotation number $F_{21}/F_{22} = 17\,711/28\,657$ ($F_{23}/F_{24} = 46\,368/75\,025$) is transformed into a periodic orbit with rotation number $F_9/F_{10} = 55/89$ ($F_{11}/F_{12} = 144/233$).

Thus, at criticality, in the vicinity of $(\hat{x}, \hat{y}) = (0, 0)$ the map is invariant under a simultaneous rescaling of spatial coordinates and rotation numbers. Since the rescaling of rotation numbers amounts to shifting the Fibonacci sequence by 12, $F_{2k+12-1}/F_{2k+12} \to F_{2k-1}/F_{2k}$, it is convenient to write the spatial scaling using factors that are powers of 12; namely, $(\hat{x}, \hat{y}) \to (\alpha^{12}\,\hat{x}, \beta^{12}\,\hat{y})$, where $\alpha = \sqrt[12]{321.92}$, $\beta = \sqrt[12]{463.82}$. In this way, the map at criticality remains invariant after 12 successive shiftings of rotation numbers $F_i/F_{i+1} \to F_{i-1}/F_i$ and 12 successive

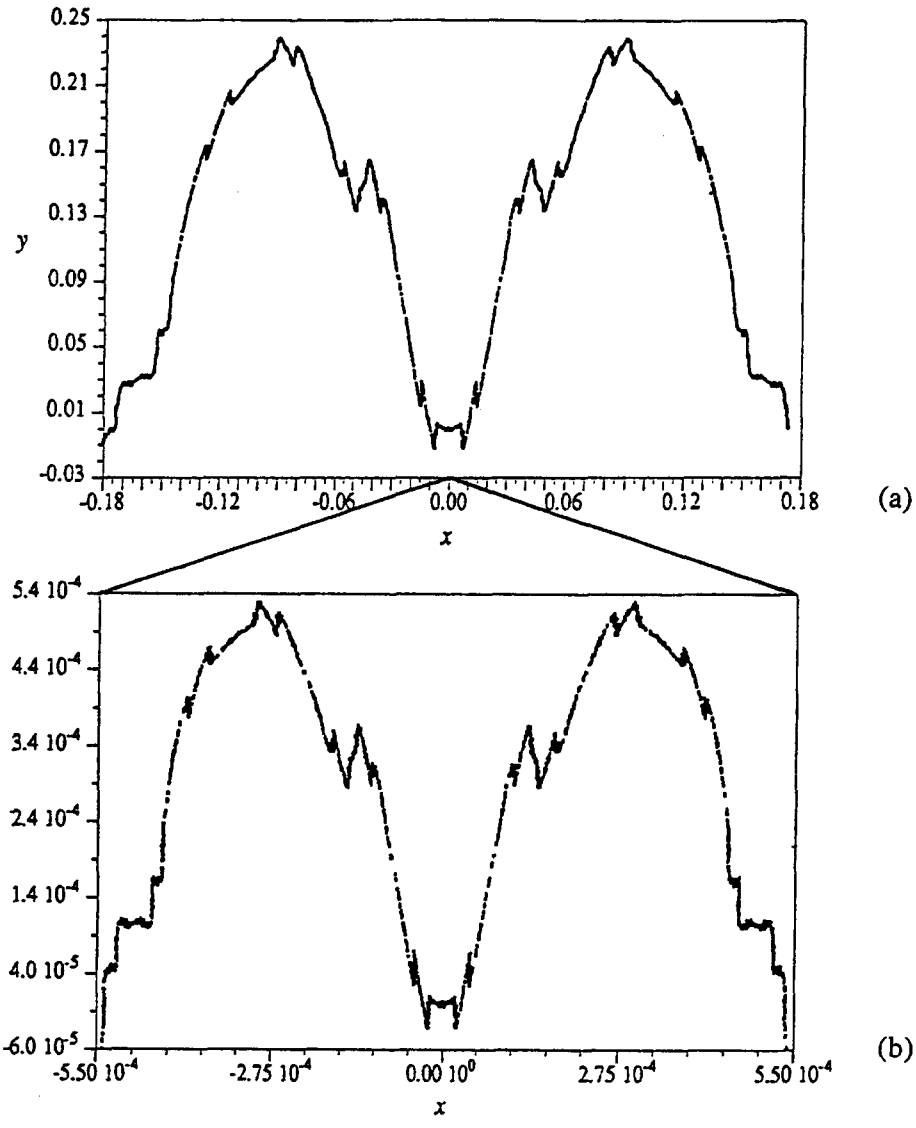

Fig. 1. Self-similar structure of the $1/\gamma$ shearless curve at criticality. In case (a) the shearless curve has been plotted in symmetry-line coordinates. Case (b) is a magnification of (a) by a factor of 321.92 in the x-direction and 463.82 in the y-direction.

spatial rescalings $(\hat{x}, \hat{y}) \to (\alpha\,\hat{x}, \beta\,\hat{y})$. In Section 3, it will be shown that this is equivalent to saying that the map at criticality is invariant under the 12th iterate of the renormalization group operator.

To formalize the previous ideas, let $(\tilde{x}_i, \tilde{y}_i)$ denote the symmetry line coordinates of the up F_{i-1}/F_i periodic orbit closest to (0, 0) (similar results are obtained using the down-periodic orbit), i.e. closest to the point where the shearless curve intersects the s_3 symmetry line. Then, in the limit $n \to \infty$, it is observed numerically that periodic orbits approach the shearless curve (i.e. $\tilde{x}$ and $\tilde{y}$ converge to zero) according to the power laws

$$\tilde{x}_{2n} = \mathcal{X}(n)\,\alpha^{-2n}, \qquad \tilde{y}_{2n} = \mathcal{Y}(n)\,\beta^{-2n}, \tag{14}$$

where $\mathcal{X}, \mathcal{Y}$ are the period-six functions ($\mathcal{X}(n+6) = \mathcal{X}(n)$ and $\mathcal{Y}(n+6) = \mathcal{Y}(n)$) shown in Table 1. Note that only

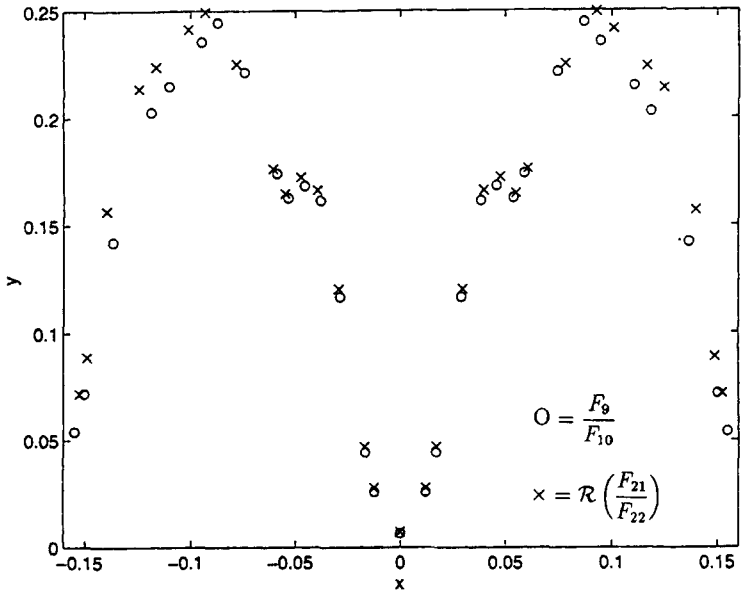

(a)

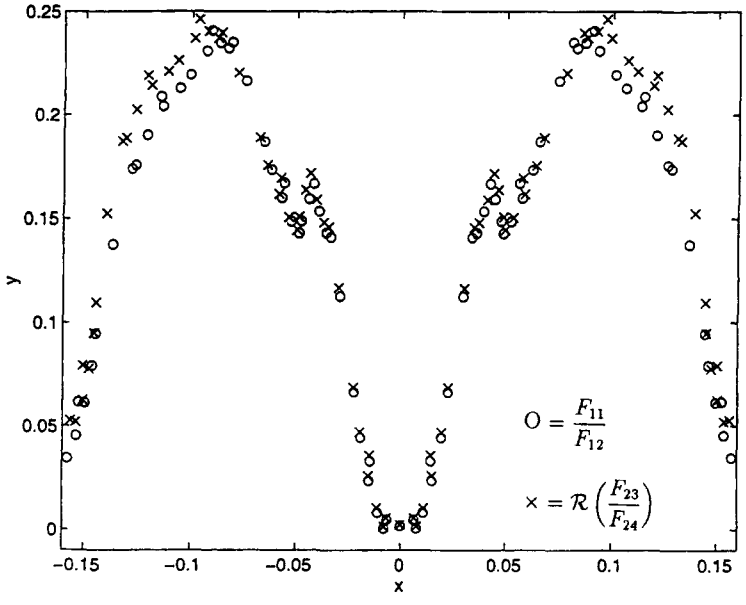

(b)

Fig. 2. Self-similar structure of periodic orbits in the standard nontwist map at criticality. In (a) the circles denote the $F_9/F_{10} = 55/89$ down periodic orbit in symmetry line coordinates, and the crosses denote the $F_{21}/F_{22} = 17\,711/28\,657$ down periodic orbits in rescaled, $(\hat{x}, \hat{y}) \to (\alpha^{12}\hat{x}, \beta^{12}\hat{y})$, symmetry line coordinates. In (b) the $F_{11}/F_{12} = 144/233$ down periodic orbits are plotted with circles along with the spatially rescaled down $F_{23}/F_{24} = 46\,368/75\,025$ periodic orbit denoted by the crosses. These two plots show that, at criticality, the periodic orbits near the symmetry line remain invariant under a simultaneous spatial rescaling and shifting of rotation numbers.

Table 1
Spatial scaling functions $\mathcal{X}$ and $\mathcal{Y}$ for up-periodic orbits

n	$\mathcal{X}(n)$	$\mathcal{Y}(n)$
1	1.303	1.387
2	1.363	2.925
3	1.306	1.073
4	1.262	1.052
5	1.516	1.105
6	2.109	0.783

coordinates $(\tilde{x}_i, \tilde{y}_i)$ with $i = 2n$ have been considered. This is because only periodic orbits with rotation numbers $\{F_{i-1}/F_i\}$ where $i = 2n$ exist. For this same reason, the exponent of α and β is $-2n$, and functions $\mathcal{X}$ and $\mathcal{Y}$ are period six, rather than period 12.

Eqs. (13), (14), and the periodicity condition on $\mathcal{Y}$ imply

$$y_s = \lim_{n\to\infty} \frac{y_{n+1}y_{n+6} - y_n\, y_{n+7}}{(y_{n+1} - y_n) - (y_{n+7} - y_{n+6})} \approx 0.2225230 \tag{15}$$

and

$$\alpha = \lim_{n\to\infty} \left| \frac{\tilde{x}_{2n}}{\tilde{x}_{2n+12}} \right|^{1/12} \approx 1.618, \qquad \beta = \lim_{n\to\infty} \left| \frac{\tilde{y}_{2n}}{\tilde{y}_{2n+12}} \right|^{1/12} \approx 1.668, \tag{16}$$

where in the calculation we have used periodic orbits with rotation numbers up to 46 368/75 025. Note that, as expected, $\alpha^{12} = 321.92$, and $\beta^{12} = 463.82$ are the scaling factors used in Fig. 1.

3. Renormalization

In Section 2, it was shown that after a spatial rescaling, at criticality, orbits with high period are mapped into orbits of lower period (as shown e.g. in Fig. 2). In this section the renormalization group formalism is used to explore this invariance in greater detail.

3.1. Renormalization group operator

Following [11–13] we define the renormalization operator for the $1/\gamma$ KAM curve in terms of pairs of commuting maps. A *pair of commuting maps* is an ordered pair of maps, (U, T), such that $UT = TU$. The orbit of a point $\boldsymbol{x}$ generated by (U, T) is the set of points $\{U^q T^p \boldsymbol{x}\}$, where q and p are integers. Given the set of periodic orbits $\{\boldsymbol{x}_i\}$ of M with rotation numbers $\{m_i/n_i\}$, the commuting map pair (U, T) associated with M is defined by the condition $U^{m_i} T^{n_i} \boldsymbol{x}_i = \boldsymbol{x}_i$. Commuting map pairs are useful because they provide a simple way for defining the renormalization group operator.

For the $1/\gamma$ KAM curve, the renormalization group operator is defined as follows [11,12]:

$$\mathcal{R}\begin{pmatrix} U \\ T \end{pmatrix} := B\begin{pmatrix} T \\ TU \end{pmatrix} B^{-1}. \tag{17}$$

This operator contains both time and space renormalization. The *space renormalization* is represented by the operator B, which rescales the (x, y) coordinates, i.e. $(x, y) \to B(x, y)$ where

$$B = \begin{pmatrix} \alpha & 0 \\ 0 & \beta \end{pmatrix}. \tag{18}$$

The values of α and β are chosen to give the appropriate magnification of the phase space in the vicinity of the $1/\gamma$ KAM curve.

The idea of *time renormalization* is to transform periodic orbits with large periods into periodic orbits with smaller periods, which amounts to a rescaling of time. To understand how Eq. (17) accomplishes this, note that:

If $\boldsymbol{x}$ is a periodic orbit of (U, T) with rotation number F_{j-1}/F_j, then $\boldsymbol{x}$ is a periodic orbit of $(\tilde{U}, \tilde{T}) = (T, TU)$ with rotation number F_{j-2}/F_{j-1}.

The proof of this result is straightforward: $\tilde{U}^{F_{j-2}}\tilde{T}^{F_{j-1}} = T^{F_{j-2}}(TU)^{F_{j-1}} = T^{F_{j-2}+F_{j-1}}U^{F_{j-1}} = U^{F_{j-1}}T^{F_j}$, where the commutation relation $TU = UT$ and the definition of the Fibonacci sequence, $F_j = F_{j-1} + F_{j-2}$, have been used. Hence, if $\boldsymbol{x}$ is a periodic orbit of (U, T) with rotation number F_{j-1}/F_j, then $U^{F_{j-1}}T^{F_j}\boldsymbol{x} = \boldsymbol{x}$, and since $U^{F_{j-1}}T^{F_j} = \tilde{U}^{F_{j-2}}\tilde{T}^{F_{j-1}}$, it is concluded that $\boldsymbol{x}$ is a periodic orbit of $(\tilde{U}, \tilde{T})$ with rotation number F_{j-2}/F_{j-1}. By induction it is apparent that an orbit with rotation number F_{j-1}/F_j under (U, T) is transformed into an orbit with rotation number F_{j-n-1}/F_{j-n} under $\mathcal{R}^n(U, T)$. Evidently $\mathcal{R}$ shifts the rotation number of the periodic orbits, an operation that is equivalent to rescaling time.

To better understand the action of $\mathcal{R}$ on the space of maps it is convenient to introduce coordinates for this domain. This is done by using the residues. A map M will be assigned coordinates $(R_{[1]}, R_{[2]}, \ldots, R_{[i]}, \ldots)$, where $R_{[i]}$ is the residue of the F_i/F_{i+1} periodic orbit of M that approximates the $1/\gamma$ KAM curve. Since the residues of a map are independent of the coordinates used, maps related by coordinate changes of the (x, y) space will have the same coordinates in the space of maps. In fact, using the residues as coordinates amounts to dividing the space of maps into equivalence classes that contain maps with the same values of the residues for the periodic orbits approximating the KAM curve under consideration. This is advantageous because the destruction of a given KAM curve only depends upon the values of the residues. Let $(\tilde{R_{[1]}}, \tilde{R_{[2]}}, \ldots \tilde{R_{[i]}}, \ldots)$ denote the coordinates of $\mathcal{R}(M)$. Since a periodic orbit of M with rotation number F_{i-1}/F_i is transformed into a periodic orbit of $\mathcal{R}(M)$ with rotation number F_{i-2}/F_{i-1}, $\tilde{R_{[i]}} = R_{[i+1]}$ for $i = 1, 2, \ldots$ Hence in residue coordinates, the renormalization operator acts simply as a shift (or translation of coordinates).

One can view the operator $\mathcal{R}$ as defining a dynamical system in the space of maps. The existence of the $1/\gamma$ KAM curve in a map M is then determined by the asymptotic behavior of $\mathcal{R}$ acting repeatedly on M. For example, if the coordinates of a map M have a tail of zeroes, i.e. if $M = (R_{[1]}, \ldots, R_{[i]}, 0, 0, 0, \ldots)$, then the sequence $\{M, \mathcal{R}M, \mathcal{R}^2M, \mathcal{R}^3M, \ldots\}$ will converge to the map $T = (0, 0, \ldots 0, \ldots)$. Since the residues of T are all zero, the $1/\gamma$ KAM curve exists in T and therefore it exists in M, which is, from a renormalization point of view, equivalent to T. This is the renormalization group interpretation of the residue criterion.

The *fixed points* of $\mathcal{R}$, which are maps invariant under the renormalization, play a crucial role in the asymptotic behavior of $\mathcal{R}$. In particular, if a map M is in the basin of attraction of a fixed point P, then $\mathcal{R}^n M \to P$ as $n \to \infty$. From the renormalization point of view, all the maps located in the basin of attraction of a fixed point are equivalent to the fixed point.

There are two kinds of fixed points: *simple* fixed points and *critical* fixed points. A simple fixed point is an integrable map, and its basin of attraction contains all the maps for which the KAM curve under study exists. The problem of KAM theory, namely the study of the persistence of invariant circles under perturbation, is translated in renormalization language as the problem of showing that the simple fixed point is an attractor of all maps in its vicinity. The critical fixed point is the map for which the KAM curve under consideration is at the threshold of its destruction, i.e. at criticality. All the maps in the basin of attraction of the critical fixed point are, from the renormalization point of view, equivalent to the fixed point and thus exhibit the same universal transition to chaos. This is the renormalization interpretation of universality.

3.2. Simple fixed point

For twist maps, the simple fixed point is a period-one orbit of the renormalization operator [12]. For nontwist maps, no period-one fixed points exist. However, a period-two orbit of the renormalization operator that corresponds to the simple fixed point does exist. This period-two fixed point is given explicitly by

$$U_+\begin{pmatrix} x \\ y \end{pmatrix} = \begin{pmatrix} x - \gamma + y^2/\gamma \\ y \end{pmatrix} \qquad T_+\begin{pmatrix} x \\ y \end{pmatrix} = \begin{pmatrix} x + 1 + y^2 \\ y \end{pmatrix} \tag{19}$$

and

$$U_-\begin{pmatrix} x \\ y \end{pmatrix} = \begin{pmatrix} x - \gamma - y^2/\gamma \\ y \end{pmatrix} \qquad T_-\begin{pmatrix} x \\ y \end{pmatrix} = \begin{pmatrix} x + 1 - y^2 \\ y \end{pmatrix}. \tag{20}$$

It is easy to check that $\mathcal{R}(U_\pm, T_\pm) = (U_\mp, T_\mp)$, and thus $\mathcal{R}^2(U_\pm, T_\pm) = (U_\pm, T_\pm)$ with

$$B = \begin{pmatrix} -\gamma & 0 \\ 0 & -\gamma \end{pmatrix}. \tag{21}$$

If $\boldsymbol{x}$ is a periodic orbit of $(U_\pm, T_\pm)$ with rotation number $w_\pm = m/n$, then by definition $U_\pm^m T_\pm^n \boldsymbol{x} = \boldsymbol{x}$ which, upon using Eqs. (19) and (20), implies $n(1 \pm y^2) + m(-\gamma \pm y^2/\gamma) = 0$. This last equation gives the following expression for the rotation number as a function of y:

$$w_\pm(y) = \frac{\gamma\left(1 \pm y^2\right)}{\gamma^2 \mp y^2}. \tag{22}$$

Accordingly, the map pairs of the period-two fixed point correspond to the following integrable nontwist maps:

$$(U_\pm, T_\pm) \Longleftrightarrow \begin{cases} x_{i+1} = x_i + w_\pm(y_{i+1}) \\ y_{i+1} = y_i. \end{cases} \tag{23}$$

Observe that at $y = 0$, as expected, $\partial w_\pm/\partial y_i = 0$ and $w_\pm = 1/\gamma$. Therefore, $(U_\pm, T_\pm)$ are nontwist maps with a shearless curve of rotation number equal to $1/\gamma$ at $y = 0$. Upon a change of coordinates the standard nontwist map of Eqs. (3) and (4) with $b = 0$ is equivalent to the map (U_-, T_-). On the other hand, for y close to zero, the map (U_+, T_+) is equivalent, up to a coordinate change, to a standard nontwist map with an "inverted shear"; i.e., to the map: $x_{i+1} = x_i + a(1 + y_{i+1}^2)$, $y_{i+1} = y_i$. Because of this, the map (U_+, T_+) ((U_-, T_-)) only possesses periodic orbits with rotation numbers greater (less) than $1/\gamma$. As said before, the simple fixed point is important because its basin of attraction contains all the nontwist maps for which the $1/\gamma$ shearless curve exists. In particular, the standard nontwist map, with (a, b) values on the $b = \Phi_{1/\gamma}(a)$ bifurcation curve and with $a < a_c$, defines a one-parameter family of nontwist maps that is in the basin of attraction of the simple fixed point.

To illustrate the invariance properties of the period-two fixed point, up and down periodic orbits of (U_-, T_-) with rotation numbers $F_5/F_6 = 8/13$ and $F_7/F_8 = 21/34$ are shown in Fig. 3. In this figure, the circles denote the coordinates of the $8/13$ periodic orbits, while the crosses denote the coordinates of the $21/34$ periodic orbits after the spatial rescaling $(x, y) \to (\gamma^2 x, \gamma^2 y)$. The figure shows that (U_-, T_-) remains invariant under the simultaneous rescaling of spatial coordinates $(x, y) \to (\gamma^2 x, \gamma^2 y)$ and of rotation numbers $F_{k+2}/F_{k+2+1} \to F_k/F_{k+1}$. Evidently, (U_-, T_-) is invariant under $\mathcal{R}^2$, since $\mathcal{R}$ rescales the rotation numbers as $F_{k+1}/F_{k+1+1} \to F_k/F_{k+1}$, and the matrix B in Eq. (21) rescales the coordinates by $-\gamma$.

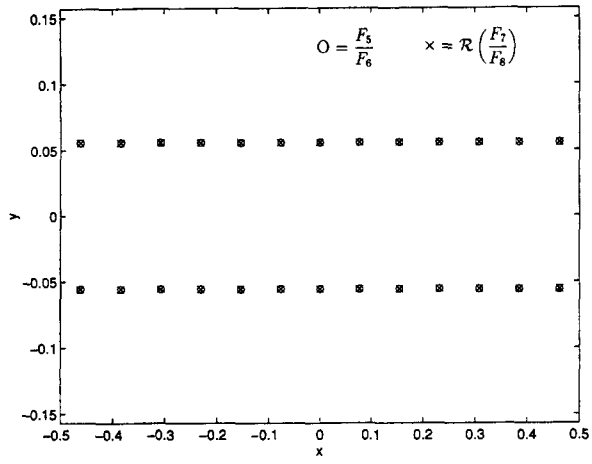

Fig. 3. Trivial self-similar structure of the integrable nontwist map. The circles denote the $F_5/F_6 = 8/13$ up and down periodic orbits, and the crosses the spatialy rescaled, $(x, y) \to (\gamma^2 x, \gamma^2 y)$, $F_7/F_8 = 21/34$ up and down periodic orbits. The plot shows that the integrable map is invariant under a simultaneous spatial rescaling and shifting of rotation numbers.

3.3. Critical fixed point

As stated before, in residue coordinates, the nth coordinate of a map M is given by the value of the residue of the periodic orbit with rotation number F_n/F_{n+1}. However, when dealing with nontwist maps, one must keep in mind that only half of the Fibonacci sequence exists; and, therefore, only half of the coordinates are available. Consider the following nontwist map

$$\Lambda = (H_1, -, H_2, -, H_3, -, H_4, -, H_5, -, H_6, -, H_1, -, H_2, -, H_3, \ldots), \tag{24}$$

where H_i are the elements of the six-cycle in Eqs. (10)–(12) and the "–" denote the missing elements of the Fibonacci sequence. By construction, this map is a period-12 fixed point of the renormalization operator, i.e.

$$\mathcal{R}^{12}\Lambda = \Lambda. \tag{25}$$

Let M_c denote the standard nontwist map at criticality, i.e. $(a, b) = (a_c, b_c)$ as given in Eq. (9). In Section 2, it was described how the residues of M_c converge asymptotically to the six-cycle $\{H_1, H_2, H_3, H_4, H_5, H_6\}$. In renormalization language this means that

$$\lim_{n\to\infty} \mathcal{R}^n M_c = \Lambda; \tag{26}$$

that is, the standard nontwist map at criticality is in the basin of attraction of the period-12 fixed point of $\mathcal{R}$.

To gain some intuition about the dynamics of $\mathcal{R}$, consider the projection onto a two-dimensional plane Π in the space of maps. Without loss of generality, Π will be taken to be the $(R_{[1]}, R_{[7]})$-plane, where $R_{[n]}$ is the residue of the $[n] = F_n/F_{n+1}$ periodic orbit of M. Accordingly, a map with coordinates $(R_{[1]}, R_{[3]}, R_{[5]}, \ldots, R_{[n]}, \ldots)$ is projected onto Π as a "point" with coordinates $(R_{[1]}, R_{[7]})$. We denote the coordinates of M restricted to Π by $M|_\Pi$. The analysis is simplified if instead of studying an orbit of $\mathcal{R}$ one considers an orbit of $\mathcal{R}^6$. Under $\mathcal{R}^6$ the critical point becomes a period-two fixed point, which is easier to visualize than the period-12 fixed point of $\mathcal{R}$.

Consider the residue coordinates of M_c that correspond to the down orbits on s_1. The coordinates of $M_c|_\Pi$ are $(2.778, -1.325)$, which are the residues of the periodic orbits of M_c with rotation numbers $1/2$ and $21/34$, respectively. Under the action of $\mathcal{R}^6$, the coordinate corresponding to the periodic orbit with rotation number $1/2$

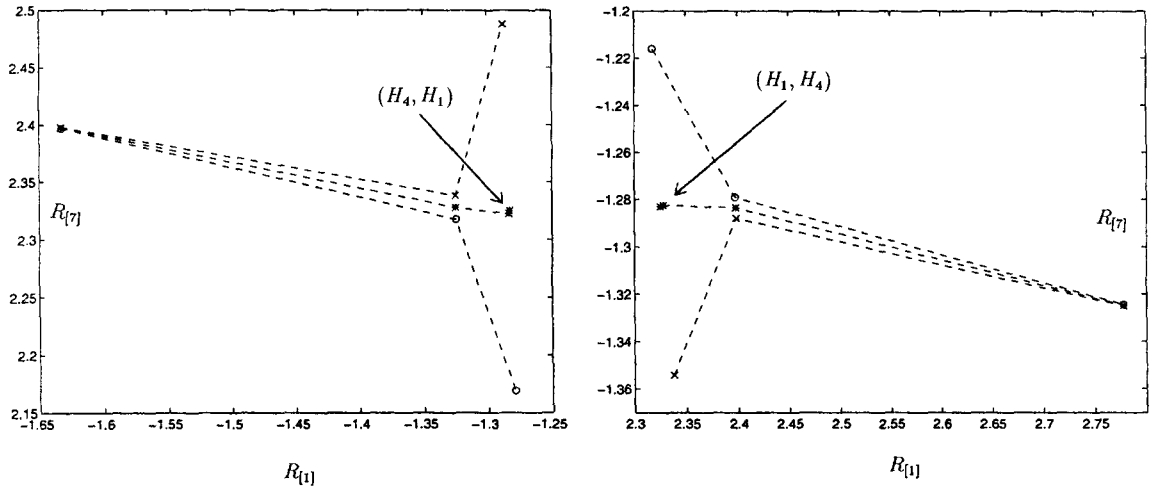

Fig. 4. Iterations of the sixth power of the renormalization group operator, $\mathcal{R}^6$, projected onto the $(R_{[1]}, R_{[7]})$ plane in the space of maps. For visualization purposes the iterations are shown in two separate panels. The stars denote the orbit of $\mathcal{R}^6$ acting on M_c, the standard nontwist map at criticality. Since M_c is in the basin of attraction of the critical period-12 fixed point of $\mathcal{R}$, the stars converge to the period-two cycle $\{(H_1, H_4), (H_4, H_1)\}$. The circles and crosses denote orbits of $\mathcal{R}^6$ acting on the standard nontwist map below and above criticality, respectively.

is transformed into that with rotation number 21/34, and the coordinate corresponding to the periodic orbit with rotation number 21/34 is transformed into that with 377/610; accordingly, $\mathcal{R}^6 M_c|_{\Pi} = (-1.325, 2.328)$, where 2.328 is the residue of the orbit with rotation number 377/610. Repeating this procedure produces a set of points of Π generated by M_c under the action of $\mathcal{R}^6$; namely,

$$\mathcal{O}^c_{s_1 d} := \{(2.778, -1.325), (-1.325, 2.328), (2.328, -1.283), \ldots\}. \tag{27}$$

Alternatively, one can consider the residues of the up periodic orbits of M_c on s_3 and construct the set $\mathcal{O}^c_{s_3 u}$. The stars of Fig. 4 denote the points of $\mathcal{O}^c_{s_1 d}$ and $\mathcal{O}^c_{s_3 u}$. For convenience we have plotted these points on two separate panels that depict separate regions of the Π-plane. Observe the convergence to the period-two orbit with coordinates $\{(-1.283, 2.325), (2.325, -1.283)\}$, which is precisely the orbit defined by the elements of the six-cycle $H_4 = -1.283$ and $H_1 = 2.325$. Thus, the set of points $\mathcal{O}^c_{s_1 d} \cup \mathcal{O}^c_{s_3 u}$ lies on the stable manifold of the fixed point. In a similar way, the unstable manifold of the fixed point can be visualized by iterating $\mathcal{R}^6$ on the standard nontwist map below and above criticality. The circles in Fig. 4 denote the orbits below criticality, while the crosses denote the orbits above criticality. These orbits were constructed by computing the residues for (a, b) values slightly below and slightly above (a_c, b_c). Observe that, as expected, below criticality iterations of the renormalization operator show a tendency towards the simple fixed point (0, 0), whereas above criticality the residues converge to (∞, ∞), which can be viewed as another simple fixed point of $\mathcal{R}$.

3.4. Eigenvalues

Now we study the renormalization group operator $\mathcal{R}$ in the vicinity of the critical fixed point A. In particular, we compute the eigenvalues that govern the rate of departure from A. Fig. 6 shows a cartoon of the infinite-dimensional space of maps in the neighborhood of A. The axes in the figure label the residues coordinates, $\mathcal{S}$ is the stable manifold, and $\mathcal{U}$ is the unstable manifold. That is, iterations of a map on $\mathcal{S}$ asymptotically approach A, whereas

iterations of a map on $\mathcal{U}$ depart from Λ. Orbits nearby $\mathcal{S}$, like those starting at P_1 and P_2 in Fig. 6, initially follow the stable manifold and then depart from Λ along the unstable manifold.

It will prove convenient to work with the 12th iterate of $\mathcal{R}$, rather than with $\mathcal{R}$ itself. Accordingly, we define

$$\hat{\mathcal{R}} := \mathcal{R}^{12}. \tag{28}$$

The critical fixed point Λ is then a period-one fixed point of $\hat{\mathcal{R}}$. Close to Λ the renormalization operator can be linearized:

$$\hat{\mathcal{R}}(\Lambda + \delta\Lambda) \approx \Lambda + D\hat{\mathcal{R}}(\Lambda) \cdot \delta\Lambda, \tag{29}$$

and if $\{\psi_i\}$ are the eigenvectors of $D\hat{\mathcal{R}}$ with eigenvalues $\{\mu_i\}$, then

$$\hat{\mathcal{R}}^n(\Lambda + \delta\Lambda) \approx \Lambda + \Sigma_i c_i \mu_i^n \psi_i, \tag{30}$$

where c_i is the projection of $\delta\Lambda$ along ψ_i. If $|\mu_i| > 1$, $\mu_i^n \to \infty$ as $n \to \infty$, and the eigenvalue is called unstable. On the other hand, if $|\mu_i| < 1$, $\mu_i^n \to 0$ as $n \to \infty$ and the eigenvalue is called stable. Following the terminology used in the theory of critical phenomena we refer to the eigenvectors with unstable eigenvalues as *relevant eigenvectors*, and to the eigenvectors with stable eigenvalues as *irrelevant eigenvectors*. Thus, only perturbations $\delta\Lambda$ with components along the relevant eigenvectors lead to departures from criticality. Since the relevant eigenvectors span the tangent space of $\mathcal{U}$ at Λ, the dimension of $\mathcal{U}$ equals the number of relevant eigenvectors. This number is closely related to the number of independent control parameters necessary to put the system at criticality. In particular, if criticality is observed at an isolated point in parameter space, then the number of relevant eigenvectors equals the number of control parameters. In the simplest case, e.g. the standard map, there is only one control parameter. However, as we have seen before, for the standard nontwist map we have to adjust two parameters in order to achieve criticality, which occurs at the isolated point (a_c, b_c). Thus, in this case, there are two relevant eigenvectors, and the unstable manifold $\mathcal{U}$ is two-dimensional as shown in Fig. 6. All maps on $\mathcal{S}$ are, upon renormalization, equivalent to Λ and therefore share all the scaling properties of Λ. For example, the spatial scaling properties of the $1/\gamma$ shearless curve in the standard nontwist map at criticality are shared by Λ, and all the maps on $\mathcal{S}$. Departures from criticality also exhibit universal scaling behavior because *all* the departures are governed by the *same* relevant eigenvectors.

The main difficulty in computing the relevant (i.e. unstable) eigenvalues of $\hat{\mathcal{R}}$ is that the space of maps is infinite-dimensional whereas the (a, b) parameter space has only two dimensions. Obviously, with only two parameters the space of maps cannot be completely explored. However, the two-dimensional unstable manifold $\mathcal{U}$ in the vicinity of Λ can be explored using (a, b) values close to (a_c, b_c). In order to do this, we define a renormalization operator in (a, b) space, $\rho(a_n, b_n) = (a_{n+1}, b_{n+1})$, such that for (a, b) close to (a_c, b_c):

$$\lim_{n\to\infty} \rho^n(a, b) = (a_c, b_c), \tag{31}$$

$$\rho(a_c, b_c) = (a_c, b_c), \tag{32}$$

and

$$\hat{\mathcal{R}}(M(\rho(a, b))) = M(a, b). \tag{33}$$

Conditions (31) and (32) mean that (a_c, b_c) is an attracting fixed point of ρ, and (33) means that ρ acting on the space of parameters is the inverse of $\hat{\mathcal{R}}$ acting on the space of maps. This last condition is the key property that will be used to compute the eigenvalues of $\hat{\mathcal{R}}$ from the eigenvalues of ρ.

Near (a_c, b_c), the operator ρ can be linearized:

$$\rho(a_c + \delta a, b_c + \delta b) \approx (a_c, b_c) + D\rho(a_c, b_c) \cdot (\delta a, \delta b), \tag{34}$$

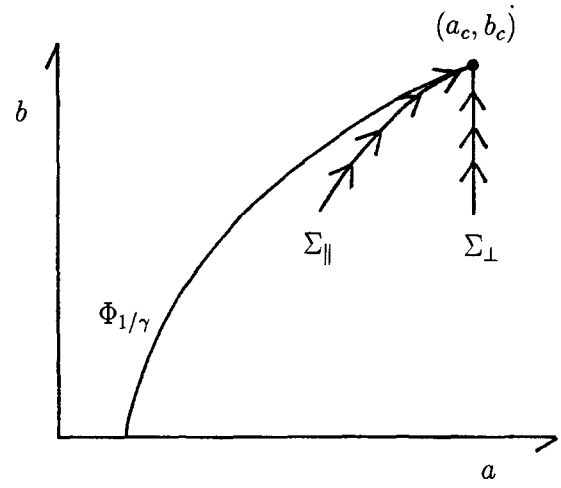

Fig. 5. Paths in (a, b) parameter space used to compute the relevant (i.e. unstable) eigenvalues. (a_c, b_c) is the critical value, and $\Phi_{1/\gamma}$ denotes the $1/\gamma$ bifurcation curve, i.e. the set of (a, b) values for which the rotation number of the shearless curve is $1/\gamma$. $\Sigma_{\perp}$, which approaches (a_c, b_c) in a direction tranverse to $\Phi_{1/\gamma}$, yields the dominant unstable eigenvalue δ_1. In the limit $(a, b) \to (a_c, b_c)$, $\Sigma_{\|}$ approaches (a_c, b_c) along $\Phi_{1/\gamma}$, and yields the second unstable eigenvalue δ_2. Maps $M(a, b)$ for (a, b) values on $\Sigma_{\perp}$ and $\Sigma_{\|}$, follow paths in the space of maps like the ones in Fig. 6 starting on P_1 and P_2, respectively.

and if ϕ_i, $i = 1, 2$, are the eigenvectors of $D\rho$ with eigenvalues ν_i, then

$$\rho\left((a_c, b_c) + \phi_i\right) \approx (a_c, b_c) + \nu_i \phi_i. \tag{35}$$

In the limit $n \to \infty$, $M(\rho^n(a, b))$ is on the unstable manifold $\mathcal{U}$ and, because of (33), there is a one-to-one correspondence between paths in (a, b) space generated by ρ, and paths in $\mathcal{U}$ generated by $\hat{\mathcal{R}}^{-1}$. This implies that the unstable eigenvalues of $\hat{\mathcal{R}}$ are the inverses of the stable eigenvalues of ρ, that is $\mu_i = 1/\nu_i$. Denoting the unstable eigenvalues of $\mathcal{R}$ by δ_1 and δ_2, it is concluded from (28) that

$$\delta_i = (1/\nu_i)^{1/12}. \tag{36}$$

To compute the eigenvalues ν_i, we will study the linear behavior of ρ along two directions in (a, b) space: one transverse and the other tangent to the $1/\gamma$ bifurcation curve at (a_c, b_c) as shown in Fig. 5.

3.4.1. *Computation of* δ_1

To compute the first eigenvalue consider the following sequence of parameter values:

$$\Sigma_{\perp} = \{(a_c, b_{[2]}),\ (a_c, b_{[3]}), \ldots (a_c, b_{[n]}), \ldots\}, \tag{37}$$

where $b_{[n]} := \Phi_{[n]}(a_c)$. (Recall $[n] = F_n/F_{n+1}$.) This sequence approaches the critical point (a_c, b_c) in a direction "perpendicular" to the $\Phi_{1/\gamma}$ bifurcation curve as shown in Fig. 5. The action of the renormalization operator ρ on this sequence is defined as

$$\rho\,(a_c, b_{[n]}) := (a_c, b_{[n+12]}). \tag{38}$$

By construction, this definition satisfies conditions (31) and (32). Condition (33) will be satisfied provided

$$\hat{\mathcal{R}}(M(a_c, b_{[2n+12]})) = M(a_c, b_{[2n]}). \tag{39}$$

Table 2
Residue invariance for δ_1

m	$R_{[2m-1]}(a_c, b_{[12]})$	$R_{[2m-1+12]}(a_c, b_{[24]})$
1	2.778	2.328
2	2.652	2.596
3	−0.759	−0.609
4	−1.334	−1.292
5	2.673	2.674
6	1.572	1.510

Table 3
Scaling function $B_\perp(n)$

n	$B_\perp(n)$	n	$B_\perp(n)$
1	1.2337	7	1.1295
2	−2.0434	8	−1.6287
3	1.8613	9	1.8445
4	−1.3599	10	−2.3512
5	1.6866	11	1.6863
6	−1.3433	12	0.3038

Denoting by $R_{[m]}(a, b)$ the residue of the F_m/F_{m+1} down periodic orbit of the standard nontwist map at (a, b), and remembering that $\hat{\mathcal{R}}$ shifts the rotation number by 12, (39) becomes

$$R_{[2m-1]}(a_c, b_{[2n]}) = R_{[2m-1+12]}(a_c, b_{[2n+12]}). \tag{40}$$

Table 2 shows the values of $R_{[2m-1]}(a_c, b_{[12]})$ and $R_{[2m-1+12]}(a_c, b_{[24]})$ for down periodic orbits for $m = 1, 2, \ldots, 6$. These values show that in the limit $n \to \infty$, $n - m$ finite, (40) is satisfied and thus ρ, as defined in (38), satisfies condition (33).

Having defined ρ on the sequence $\Sigma_\perp$, let us study the linear behavior of ρ along this sequence. It is observed numerically that in the limit $n \to \infty$,

$$b_{[n+1]} = b_c + B_\perp(n)\, \nu_1^{n/12}, \tag{41}$$

a result that is accurate, for $n > 20$, to 11 significant figures. In Eq. (41) $B_\perp(n)$ is the period-12 function, $B_\perp(n+12) = B_\perp(n)$, given in Table 3, b_c is the critical b-coordinate of (9) and

$$\nu_1 = \lim_{n\to\infty} \left(\frac{b_{[n+12]} - b_c}{b_{[n]} - b_c} \right). \tag{42}$$

From Eq. (42) we have that for large n,

$$b_{[n+12]} \approx b_c + \nu_1\, (b_{[n]} - b_c). \tag{43}$$

Using this expression in (38) yields

$$\rho(a_c, b_{[n]}) \approx (a_c, b_c) + \nu_1\, (0, b_{[n]} - b_c), \tag{44}$$

thus, according to (35), $(0, b_{[n]} - b_c)$ is an eigenvector of ρ with eigenvalue ν_1. From (42) with $n = 12$, and (36) the following estimate for the first unstable eigenvalue of $\mathcal{R}$ is obtained:

$$\delta_1 \approx 2.683. \tag{45}$$

This eigenvalue gives the rate of departure from Λ for (a, b) values off the $1/\gamma$ bifurcation curve. Next we compute the second eigenvalue giving the rate of departure from (a_c, b_c) for (a, b) values along the $1/\gamma$ curve.

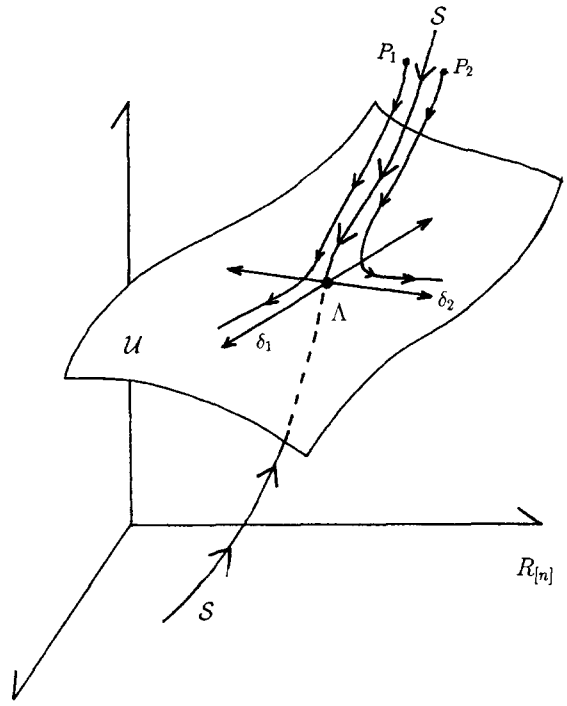

Fig. 6. Cartoon illustrating the dynamics of the twelfth iterate of the renormalization group operator, $\hat{\mathcal{R}}$, in the neighborhood of the critical fixed point, Λ, in the infinite-dimensional space of maps. The axes label the residue coordinates. $\mathcal{U}$ is the two-dimensional unstable manifold, whose tangent space at Λ is spanned by the two relevant eigenvectors with unstable eigenvalues δ_1, and δ_2. $\mathcal{S}$ is a codimension-two manifold containing all the nontwist maps for which the $1/\gamma$ shearless curve is critical. This infinite-dimensional manifold defines a universality class for the transition to chaos in nontwist maps. Maps near $\mathcal{S}$, like P_1 and P_2, initially follow $\mathcal{S}$ and then depart from Λ along $\mathcal{U}$.

3.4.2. *Computation of* δ_2

To compute the second eigenvalue we have to approach (a_c, b_c) following a sequence of (a, b) parameter values such that the corresponding path, $M(a, b)$, in the space of maps, leaves Λ along the direction of the second eigenvector as, for example, the trajectory that starts at P_2 in Fig. 6. It is natural to expect that parameter values approaching (a_c, b_c) along the $1/\gamma$ bifurcation curve, $b = \Phi_{1/\gamma}(a)$, satisfy this condition. That is, as $a \to a_c$, $M(a, \Phi_{1/\gamma}(a))$ leaves Λ along the direction of the second eigenvector. In terms of the operator ρ this means that the tangent of the $1/\gamma$ bifurcation curve at (a_c, b_c) is an eigenvector of ρ, and that there is a correspondence between (a, b) points on $\Phi_{1/\gamma}$ close to (a_c, b_c), and points on the unstable manifold generated by the second eigenvector.

Thus, following a similar approach to the one used before, we compute the second eigenvalue δ_2 by studying the standard nontwist map for (a, b) values on $\Phi_{1/\gamma}$ close to (a_c, b_c). However, in this case the problem is much harder because in practice it is necessary to compute the $1/\gamma$ bifurcation curve to extreme accuracy, otherwise the first eigenvalue dominates the result. That is, if the (a, b) values are not close enough to the $1/\gamma$ bifurcation curve, the departure of $M(a, b)$ from Λ under the renormalization operator will have a dominant component along the direction of the first eigenvector. The strong effect of the first eigenvalue is one of the reasons why it is so difficult to compute the critical parameter value (a_c, b_c). In fact for (a_c, b) with $b = \Phi_{[24]}(a_c)$ ($[24] = 75,025/121,393$, $|[24] - 1/\gamma| \sim 10^{-11}$) the evolution of $M(a_c, b)$ under $\mathcal{R}$ is dominated by the first eigenvalue, even though (a_c, b) is very close to the $1/\gamma$ bifurcation curve. This is the reason why, as explained in [8], to compute (a_c, b_c), that is to have $M(a_c, b_c)$ on the stable manifold $\mathcal{S}$, it is necessary to compute b_c to 12 digit accuracy.

Table 4
Residue invariance for δ_2

m	$R_{\lfloor m \rfloor}(a_c^{[4]}, b_c^{[4]})$	$R_{\lfloor m+12 \rfloor}(a_c^{[16]}, b_c^{[16]})$
5	0.5435	0.5241
6	0.1479	0.1474
7	0.3397	0.3165
8	0.2083	0.1938
9	0.2799	0.2429
10	0.2340	0.1887
11	0.2610	0.1820

Since finding a sequence of (a, b) parameter values that are exactly on $\Phi_{1/\gamma}$ is difficult, we will use an approximate sequence, namely (a, b) values on F_{2n}/F_{2n+1} bifurcation curves for $n = 1, 2, \ldots$ In the limit $n \to \infty$, this sequence approaches (a_c, b_c) along $\Phi_{1/\gamma}$ as shown in Fig. 5. Note that for these parameter values, there are two $1/\gamma$ KAM curves, the so-called up and down curves. Thus we will consider the sequence

$$\Sigma_{\parallel} = \{(a_c^{\lfloor 2 \rfloor}, b_c^{\lfloor 2 \rfloor}), (a_c^{\lfloor 4 \rfloor}, b_c^{\lfloor 4 \rfloor}), \ldots, (a_c^{\lfloor 2n \rfloor}, b_c^{\lfloor 2n \rfloor}), \ldots\}, \tag{46}$$

where for $n = 1, 2, \ldots$, $(a_c^{\lfloor 2n \rfloor}, b_c^{\lfloor 2n \rfloor})$ is the point on the F_{2n}/F_{2n+1} bifurcation curve at which the up (and down) $1/\gamma$ KAM curve is critical. The renormalization operator ρ acting on this sequence is defined as

$$\rho(a_c^{\lfloor 2n \rfloor}, b_c^{\lfloor 2n \rfloor}) := (a_c^{\lfloor 2n+12 \rfloor}, b_c^{\lfloor 2n+12 \rfloor}). \tag{47}$$

This definition clearly satisfies (31) and (32), and condition (33) will be fulfilled provided

$$R_{\lfloor m \rfloor}(a_c^{\lfloor 2n \rfloor}, b_c^{\lfloor 2n \rfloor}) = R_{\lfloor m+12 \rfloor}(a_c^{\lfloor 2n+12 \rfloor}, b_c^{\lfloor 2n+12 \rfloor}). \tag{48}$$

Table 4 shows numerical evidence that support the validity of this relation.

Having defined ρ we turn now to the problem of studying the behavior of ρ near (a_c, b_c). In the limit $n \to \infty$, the $\{a_{\lfloor 2n \rfloor}\}$ sequence satisfies the scaling relation

$$a_c^{\lfloor 2n \rfloor} = a_c + A_{\parallel}(n)\, \nu_2^{n/6}, \tag{49}$$

where $A_{\parallel}(n)$ is a period-six function, $A_{\parallel}(n+6) = A_{\parallel}(n)$, a_c is the critical a-coordinate of (9), and

$$\nu_2 = \lim_{n\to\infty} \left(\frac{a_c^{\lfloor 2n+12 \rfloor} - a_c}{a_c^{\lfloor 2n \rfloor} - a_c} \right). \tag{50}$$

Thus, for large n

$$a_c^{\lfloor 2n+12 \rfloor} \approx a_c + \nu_2\, (a_c^{\lfloor 2n \rfloor} - a_c). \tag{51}$$

On the other hand, the b values scale as

$$b_c^{\lfloor 2n \rfloor} = \Phi_{1/\gamma}(a_c^{\lfloor 2n \rfloor}) + B_{\parallel}(n)\, \tilde{\nu}_1^{n/6}, \tag{52}$$

where $B_{\parallel}$ is a period-six function, and

$$\tilde{\nu}_1 = \lim_{n\to\infty} \left(\frac{b_c^{\lfloor 2n+12 \rfloor} - \Phi_{1/\gamma}\left(a_c^{\lfloor 2n+12 \rfloor}\right)}{b_c^{\lfloor 2n \rfloor} - \Phi_{1/\gamma}\left(a_c^{\lfloor 2n \rfloor}\right)} \right). \tag{53}$$

Accordingly, for large n

$$b_c^{[2n+12]} \approx b_c + \tilde{\nu}_1 (b_c - \Phi_{1/\gamma}(a_c^{[2n]})). \tag{54}$$

From (51) and (54), we then conclude that for large n

$$\rho(a_c^{[2n]}, b_c^{[2n]}) \approx (a_c, b_c) + \tilde{\nu}_1 (0, b_c - \Phi_{1/\gamma}(a_c^{[2n]})) + \nu_2 (a_c^{[2n]} - a_c, 0). \tag{55}$$

As discussed before, the eigenvalues of $\mathcal{R}$ are related to those of ρ by (36). The approximate value of $\tilde{\nu}_1$ as determined from (53) gives, using (36), $\tilde{\delta} \approx 2.748$, which within numerical error equals δ_1. Thus, the second term on the right-hand side of (55) is the component along the previously found eigenvector. This component is not zero in this case because the sequence $\Sigma_{\parallel}$ is not exactly on $\Phi_{1/\gamma}$. On the other hand, the third term of (55) gives the projection of the departure from Λ along the second eigenvector, whose eigenvalue according to (50) has the approximate value

$$\delta_2 \approx 1.511. \tag{56}$$

4. Conclusions

In this paper we have presented a renormalization group study of the transition to chaos in area preserving nontwist maps, maps that violate the twist condition. These maps represent a type of degenerate Hamiltonian system. They occur in many applications: chaotic transport in fluid dynamics, reversed shear discharges in tokamak plasmas, and trajectories about oblate planets in celestial mechanics, to name a few. From a mathematical point of view, nontwist maps are interesting because, as mentioned before, most of the theorems (including the KAM theorem) assume the twist condition; many well-known and powerful results for area preserving maps remain to be proved for nontwist maps.

The present work was based on the study of the standard nontwist map, a prototype nontwist map that violates the twist condition along a curve called the shearless curve. In [7,8] the critical parameter values for the destruction of the shearless curve with rotation number equal to the inverse golden mean $1/\gamma = \frac{1}{2}(1 - \sqrt{5})$ were computed, and it was shown that, at criticality, the residues converge to a period-six cycle. The objective of the present paper was to analyze these results in the renormalization group framework.

Following a review of our previous results, the spatial scaling properties of the $1/\gamma$ shearless curve were studied. It was shown that, at criticality, the shearless curve is invariant under the spatial rescaling $(\hat{x}, \hat{y}) \to (\alpha^{12}\hat{x}, \beta^{12}\hat{y})$ where $\alpha \approx 1.618$, and $\beta \approx 1.668$. It was also shown that periodic orbits (in the vicinity of the symmetry line) remain invariant under the simultaneous spatial rescaling, $(\hat{x}, \hat{y}) \to (\alpha^{12}\hat{x}, \beta^{12}\hat{y})$, and shifting of rotation numbers, $F_{2k+12-1}/F_{2k+12} \to F_{2k-1}/F_{2k}$.

Two fixed points of the renormalization group operator, associated with the transition to chaos in nontwist maps, were obtained: the simple period-two fixed point and the critical period-12 fixed point. An explicit expression for the simple fixed point was presented. This fixed point corresponds to integrable nontwist maps and its basin of attraction contains all those maps for which the shearless curve exists. The critical fixed point corresponds to a nontwist map at criticality, and its basin of attraction defines a new universality class for the transition to chaos. The standard nontwist map at the critical parameter values is in the basin of attraction of this critical fixed point and is thus representative of the new universality class. Finally, the unstable eigenvalues of the period-12 fixed point were computed. Since the parameter space is two-dimensional, there are two different directions available for departure from criticality, and therefore, there are the two unstable eigenvalues: $\delta_1 \approx 2.683$ and $\delta_2 \approx 1.511$.

We note that other high-order critical fixed points are likely to exist. In particular, for nontwist maps with $x_{i+1} = x_i + a(1 - y_{i+1}^p)$, $p \neq 2$, different transition scenarios and thus other critical fixed points are expected. Also, as in

the case of twist maps [15,19,21], it is expected that perturbation functions other than $\sin(2\pi x_i)$ will yield different results. In critical phenomena, there are general geometric criteria, like dimension and symmetry, that allow the classification of the different universality classes. Unfortunately, in maps the problem is more complicated, and the criteria that go into the classification of the different universality classes are not known in general.

Acknowledgements

This work was funded by the US Department of Energy under No. DE-FG05-80ET-53088. DdCN acknowledges partial support by the Universidad Nacional Autonoma de México, and the University Corporation for Atmospheric Research Postdoctoral Program in Ocean Modeling.

References

[1] R.S. MacKay and J.D. Meiss, eds., Hamiltonian Dynamical Systems: A Reprint Selection (Adam-Hilger, London, 1987).
[2] J.D. Meiss, Rev. Mod. Phys. 64 (1992) 795.
[3] L. E. Reichl, The Transition to Chaos in Conservative Classical Systems: Quantum Manifestations (Institute for Nonlinear Science, Springer, New York, 1992).
[4] D. del-Castillo-Negrete and P.J. Morrison, Phys. Fluids A 5 (1993) 948.
[5] J. Moser, Nach. Akad. Weiss. Gottingen, Math. Phys. K1 IIa (1962) 1.
[6] R. de la Llave, private communication.
[7] D. del-Castillo-Negrete, Dynamics and transport in rotating fluids and transition to chaos in area preserving nontwist maps, Ph.D. Thesis, The University of Texas, Austin, (1994).
[8] D. del-Castillo-Negrete, J.M. Greene and P.J. Morrison, Area preserving nontwist maps: Periodic orbits and transition to chaos, Physica D 91 (1996) 1–23.
[9] L.P. Kadanoff, Phys. Rev. Lett. 47 (1981) 1641.
[10] S.J. Shenker and L.P. Kadanoff, J. Stat. Phys. 27 (1982) 631.
[11] R.S. MacKay, Renormalization in area preserving maps, Thesis, Princeton (1982) (University Microfilms Int., Ann Arbor, MI).
[12] R.S. MacKay, Physica D 7 (1983) 283.
[13] J.M. Greene, The status of KAM theory from a physicist's point of view, in: Chaos in Australia, eds. Gavin Brown and Alex Opie (World Scientific, Singapore, 1993) p. 8.
[14] J.M. Greene, H. Johannesson, B. Schaub and H. Suhl, Phys. Rev. A 36 (1987) 5858.
[15] J. Wilbrink, Physica D 26 (1987) 358.
[16] J. Wilbrink, Phys. Lett. A 131 (1988) 251.
[17] J.A. Ketoja and R.S. MacKay, Physica D 35 (1989) 318.
[18] J. Wilbrink, Nonlinearity 3 (1990) 567.
[19] J.M. Greene and J. Mao, Nonlinearity 3 (1990) 69.
[20] J.M. Greene, J. Math. Phys. 20 (1979) 1183.
[21] B. Hu, J. Shi and S.Y. Kim, J. Stat. Phys. 62 (1991) 631.